Published in final edited form as:
Circulation. 2009 August 11; 120(6): 467–476. doi:10.1161/CIRCULATIONAHA.108.825091.

Termination of atrial fibrillation using pulsed low-energy far-field stimulation

Flavio H. Fenton, PhD[*,†,1], **Stefan Luther, PhD**[*,†,2], **Elizabeth M. Cherry, PhD**[1], **Niels F. Otani, PhD**[1], **Valentin Krinsky, PhD**[3], **Alain Pumir, PhD**[4], **Eberhard Bodenschatz, PhD**[2,5], and **Robert F. Gilmour Jr., PhD**[1]

[1]Department of Biomedical Sciences, Cornell University, Ithaca, NY 14853, USA

[2]Max Planck Institute for Dynamics and Self-organization, Am Fassberg 17, D-37077 Göttingen, Germany

[3]Institute Non Lineáire de Nice, 1361 Route des Lucioles, F-06560 Valbonne, France

[4] Laboratoire de Physique, Ecole Normale Supérieure de Lyon, 06007 Lyon, France

[5]Laboratory of Solid State Physics and Department of Mechanical and Aerospace Engineering, Cornell University, Ithaca, NY 14851, USA

Abstract

Background—Electrically-based therapies for terminating atrial fibrillation (AF) currently fall into two categories: anti-tachycardia pacing (ATP) and cardioversion. ATP utilizes low-intensity pacing stimuli delivered via a single electrode and is effective for terminating slower tachycardias, but is less effective for treating AF. In contrast, cardioversion uses a single high-voltage shock to terminate AF reliably, but the voltages required produce undesirable side effects, including tissue damage and pain. We propose a new method to terminate AF called far-field anti-fibrillation pacing (FF-AFP), which delivers a short train of low-intensity electrical pulses at the frequency of ATP, but from field electrodes. Prior theoretical work has suggested that this approach can create a large number of activation sites ("virtual" electrodes) that emit propagating waves within the tissue without implanting physical electrodes and thereby may be more effective than point-source stimulation.

Methods and Results—Using optical mapping in isolated perfused canine atrial preparations, we show that a series of pulses at low field strength (0.9-1.4 V/cm) is sufficient to entrain and subsequently extinguish AF with a success rate of 93 percent (69/74 trials in 8 preparations). We further demonstrate that the mechanism behind FFAFP success is the generation of wave emission sites within the tissue by the applied electric field, which entrains the tissue as the field is pulsed.

Conclusions—AF in our model can be terminated by FF-AFP using only 13% of the energy required for cardioversion. Further studies are needed to determine whether this marked reduction in energy can increase the effectiveness and safety of terminating atrial tachyarrhythmias clinically.

†**Corresponding authors:** Flavio H. Fenton Department of Biomedical Sciences T7 012C Veterinary Research Tower College of Veterinary Medicine Cornell University Ithaca, NY 14853 Phone: 607-253-3075 Fax: 607-253-3851 fhf3@cornell.edu Stefan Luther Max Planck Institute for Dynamics and Self-organization Am Fassberg 17, D-37077 Göttingen Germany Phone: +49 551-5176-370 stefan.luther@ds.mpg.de.

*F.H.F. and S.L. contributed equally to this work.

Disclosures

None.

Keywords

arrhythmia; atrium; cardioversion; fibrillation; mapping

Atrial fibrillation (AF) is the most common sustained cardiac arrhythmia worldwide,[1] affecting more than 2.2 million people in the United States alone.[2] Complications associated with chronic AF include increased risk for both thromboembolism and stroke.[2] Left untreated, paroxysmal AF often progresses to permanent AF, which is resistant to therapy.[3] Although underlying anatomic or pathophysiologic factors may fuel this progression,[3] AF itself may lead to its own perpetuation through electrical, structural, and metabolic remodeling of atrial tissue. The realization that AF begets AF[4] has led to management strategies that are designed to avoid the progression of AF by reducing the frequency and duration of AF episodes.

One such strategy, cardioversion, attempts to reset all electrical activity in the atria and requires the use of large (>5 V/cm) electric field gradients.[5-7] These high energies cause pain and trauma for the patient, damage the myocardium and reduce battery life in implanted devices.[8] Another strategy, anti-tachycardia pacing (ATP), seeks to avoid the development of permanent AF by suppressing paroxysmal AF. ATP consists of a train of 8-10 low-energy stimuli delivered as a pacing ramp or burst at 50Hz via a single pacing electrode.[9] ATP is effective in treating spontaneous atrial tachyarrhythmias, especially slower tachycardias,[9-10] but it is not very effective for converting AF.[9,11-12]

To overcome the limitations of ATP and cardioversion, we propose a new technique that employs a series of low-amplitude pulsed electric fields to overdrive atrial fibrillation and thereby terminate it, a strategy suggested by previous experimental studies using physically implanted electrodes.[13,14] The technique, which we call far-field antifibrillation pacing (FF-AFP), takes advantage of the fact that following an electric field pulse, virtual electrodes may arise at interfaces separating regions with different conductivities.[15] These sites may be macroscopic, such as blood vessels or ischemic regions, or smaller-scale discontinuities, including areas of fibrosis or abrupt changes in fiber direction. [16-21] Virtual electrodes may become a secondary source (i.e., a site of wave emission), depending on the extent of the conductivity discontinuity and the electric field strength.

Here we use a combination of computer simulations and experiments in isolated perfused canine cardiac preparations to demonstrate that FF-AFP can terminate AF with a high success rate, even at low energies. We further show that the method is successful because the electric field creates many activation sites in the vicinity of endogenous conductivity discontinuities, [16-21] which in turn produce propagating waves, as predicted by previous studies.[22-25] Given that the virtual electrodes created by field stimulation substitute for multiple physically-implanted electrodes, this approach promises to provide a means of suppressing atrial tachyarrhythmias less invasively and with less physical and psychological trauma than with currently available therapy.

Materials and Methods

Tissue preparation

Studies were performed using hearts obtained from adult mongrel dogs of either sex weighing 10 to 30 kg. The experimental procedures were approved by the Institutional Animal Care and Use Committee of the Center for Animal Resources and Education at Cornell University. The dogs were anesthetized with Fatal-Plus (390 mg/mL pentobarbital sodium; Vortex Pharmaceuticals; 86 mg/kg IV) and their hearts excised rapidly. The right coronary artery was cannulated using polyethylene tubing and the right atrial and ventricular myocardium perfused

by that artery were excised and suspended in a heated (37°C) transparent tissue chamber where they were both perfused and superfused with normal Tyrode solution. Following 15-30 minutes of equilibration, the preparation was stained with the voltage-sensitive dye Di-4-ANEPPS (10 μM bolus). Blebbistatin (10 μM constant infusion over 30-40 minutes) was added to prevent motion artifact.[26] Arrhythmias were induced by applying ACh (1-4 μM) and initiating burst pacing with a frequency of 40Hz and amplitude of 8V.[27] Different concentrations of ACh produced a range of arrhythmias having dominant periods between 30 and 65 ms, which provided an opportunity to create arrhythmias that simulated atrial tachycardia, atrial flutter and AF in an intact heart. If shocks were not applied, AF was persistent (maximum time tracked was two hours). Field stimulating electrodes consisted of 1 cm × 5 cm^2 platinum plates embedded in epoxy and were placed on either side of the preparation 10 cm apart. Pacing and far-field stimuli consisted of rectangular pulses delivered, respectively, using a stimulator and stimulus isolator (World Precision Instruments) and a function generator (Agilent 33220A) coupled to a power amplifier (Kepco BOB 100-4M) capable of delivering field strengths from 0.01 to 4.6V/cm at cycle lengths as short as 30 ms. The field strength between the electrodes was measured using two Teflon-coated silver wires 5-7 cm apart and immersed in the bath. Tissue cryoablation was performed by pressing a metal circle or rectangle previously frozen in liquid nitrogen against the tissue surface for approximately 1 minute.

Optical mapping

Excitation light was produced by 16 high-performance light-emitting diodes (Luxeon III star, LXHL-FM3C, wavelength 530 ± 20 nm) driven by a low-noise constant-current source. The illumination efficiency was significantly enhanced by collimator lenses (Luxeon, LXHL-NX05). The fluorescence emission light was collected by a Navitar lens (DO-2595, focal length 25 mm, F/# 0.95), passed through a long-pass filter (<610 nm), and imaged by a 128×128 back-illuminated EMCCD array (electron-multiplied charge coupled device, Photometrics Cascade 128+). The signal was digitized with a 16bit A/D converter at a frame rate of 511 Hz (full frame, 128×128 pixels). The PCI interface provided high-bandwidth uninterrupted data transfer to the host computer. The instantaneous dominant frequency of an arrhythmia was obtained in real time by calculating the FFT of the signal recorded from 1 pixel in the center of the preparation in real time.

FF-AFP and cardioversion protocols

For the FF-AFP experiments, a sequence of either 5 or 10 pulses was applied with a 5-ms pulse duration and a cycle length 5-10 ms below the dominant cycle length of the arrhythmia. The electrical activation of the atria was recorded as described above and the optical activation pattern was then characterized and its dependency on stimulation energy calculated. A series of recordings was made in each experiment, with each recording lasting up to 15 seconds in duration. Field strength was varied and applied from the threshold level of activation (0.25 V/cm), as determined prior to arrhythmia induction, until arrhythmia termination was achieved or the maximal deliverable field strength was reached (~ 4.6V/cm)

Computer simulations

Computer simulations were performed using a bidomain model (Eq.1) subject to no-flux boundary conditions, with irregular boundaries handled using either a finite-volume formulation or a phase-field method.[28] Forward Euler with GMRes was used to solve the bidomain equations:

$$\begin{aligned} C_m \partial (\boldsymbol{V_i} - \boldsymbol{V_e}) / \partial t &= \nabla D_i \nabla (\boldsymbol{V_i} - \boldsymbol{V_e}) - \boldsymbol{J_{ion}} \\ C_m \partial (\boldsymbol{V_i} - \boldsymbol{V_e}) / \partial t &= -\nabla D_e \nabla (\boldsymbol{V_i} - \boldsymbol{V_e}) + \boldsymbol{J_{ion}} \end{aligned} \quad \text{Eq. 1}$$

where $\boldsymbol{V_i}$ and $\boldsymbol{V_e}$ are the intracellular and extracellular potentials, the membrane potential is given by $\boldsymbol{V_m}=\boldsymbol{V_i}-\boldsymbol{V_e}$, and the intra- and extracellular diffusions are given by D_i and D_e. The membrane dynamics is given by the ionic current density $\boldsymbol{J_{ion}}$. Two realistic ionic models were used.[29,30] In some cases, the insulating plaque that typically forms between myocardial fibers in older hearts[31] was modeled by randomly removing gap junctions along short lines (average length 625 μm) oriented along the fiber direction (average spacing 2.5 mm). Atrial simulations included the ACh-activated K^+ current.[32] Less intense computations were performed on a desktop computer, whereas larger computations were performed on a 4136-processor Cray XT3 MPP machine at the Pittsburgh Supercomputing Center.

Statistics

Data are expressed as mean +/- standard error. Statistical significance was determined by comparing the log of the ratio of the FF-AFP energy requirement and the standard defibrillation energy requirement using Restricted Maximum Likelihood estimates for a random effects model implemented in the JMP statistical package. Because multiple trials were performed in individual preparations, a random effects model was used to account for the correlation of observations from the same preparation. $p<0.05$ was considered significant.

Results

Termination of atrial arrhythmias with FF-AFP

Prior theoretical work[24] has suggested that low-energy cardioversion may be possible by applying a pulsed electric field. To test this hypothesis, we induced sustained arrhythmias in excised canine atrial tissue preparations, applied a pulsed electric field, and used optical mapping to record the electrical activity before and after delivery of the field. Fig. 1a-d and the related movie shows an example of successful AF termination via FF-AFP. Optical signals for the mapped atrium, along with the signal recorded from one pixel during AF are shown, with the light blue shaded regions indicating the time during which far-field pulses of 1.4 V/cm were delivered at a cycle length of 45 ms. Complex non-repeating electrical wave patterns that characterize AF were seen before application of FF-AFP shocks (Fig. 1b). The initial FF-AFP shock entrained only part of the tissue (first panel in Fig.1c), whereas subsequent shocks entrained progressively more tissue until the entire mapped area was activated by the last shock (last panel in Fig. 1c). After delivery of five shocks, the arrhythmia terminated and full repolarization and quiescence ensued (Fig. 1d). An additional example of successful conversion of AF in a different preparation can be seen in Fig. 2a and the related movie. In this case, successful termination occurred after the delivery of five far-field pulses of 1.63 V/cm at a cycle length of 40 ms.

If the electric field strength was too low, an insufficient number of activation sites were recruited and only partial entrainment occurred, resulting in an unsuccessful defibrillation attempt, as shown in Fig. 1e-h and the related movie. Although the lower field strength of 0.9 V/cm altered activation patterns during AF and even changed the chirality of the reentry (compare Fig. 1f and Fig. 1h), it did not fully entrain the tissue. Consequently, the arrhythmia persisted. Fig. 2b and the related movie show another unsuccessful defibrillation attempt using a field strength of 1.40 V/cm in the same preparation as Fig. 2a.

FF-AFP was effective over a broad range of dominant arrhythmia periods (30-65 ms) generated using different concentrations of ACh (1-4 μM), as illustrated in Fig. S1, which shows optical signals from one pixel for six different arrhythmia episodes successfully terminated using FFAFP (field strength 1.40 V/cm). In a total of 74 trials in 8 preparations, FF-AFP terminated 69 episodes of AF, resulting in a 93 percent success rate. Of those 69 episodes, 45 were terminated using a single series of 5 pulses, and 24 required additional attempts (up to a

maximum of four). Each of the preparations used for these studies contained a large enough portion of the right ventricle to support ventricular fibrillation (see Fig. S2 and the related movie), but in no case did FF-AFP induce ventricular fibrillation.

Energy reduction achieved by terminating atrial arrhythmias with FF-AFP compared to a single shock

For comparison, in 12 trials in 4 preparations, the electric field strengths required to terminate AF using FF-AFP were compared with those required to terminate AF using a single shock (akin to standard cardioversion). Fig. 3 and the related movie shows an example of an episode of AF that could not be defibrillated by a single strong shock of 4.67 V/cm applied for 5 ms, comparable to the 5 V/cm typically required for cardioversion.[5] To terminate AF in this preparation using a single shock, it was necessary to apply a minimum electric field strength of 3.73 V/cm for 10 ms, with a corresponding energy of 4.26 J, as shown in Fig. 4 and the related movie. In comparison, each FF-AFP shock in the successful defibrillation shown for the same preparation in Fig. 4 required only 0.4 J, a reduction in energy of 91 percent. Overall, the average energy required for defibrillation using FF-AFP was 12.4±1.9 percent of that required for a single shock ($p<0.002$).

FF-AFP mechanism: Generation of activation sites within the tissue

We hypothesized that FF-AFP terminates AF by synchronizing tissue activation. Synchronization occurs because the pulsed electric fields create virtual electrodes at conductivity discontinuities, which results in the activation of increasingly larger regions of tissue with successive pulses.

To test this idea, we first determined the response to a single electric field pulse in quiescent tissue. Fig. 5a illustrates schematically how an activation site develops upon application of an electric field in a one-dimensional circuit representation of cardiac tissue containing a generic conductivity discontinuity between myocardium and an inexcitable obstacle. Three separate interfaces between excitable and inexcitable regions are included: the single obstacle and the two tissue edges. When an electric field is applied, current flows out from the positive electrode through the extracellular medium and enters the tissue at the tissue edge and subsequently exits at the boundary of the inexcitable region. Similarly, on the other side of the inexcitable region, current reenters the tissue at the boundary and exits at the tissue edge. In quiescent tissue, this current produces depolarization (hyperpolarization), shown in red (blue), in the conducting region along all interface boundaries where the excitable tissue is closer to the positive (negative) electrode. The resulting virtual electrodes[16-23] alter electrical activity in the tissue without the presence of a physical electrode. If the depolarized region reaches the threshold for excitation, it can initiate propagating waves, thereby serving as an activation site, also known as a secondary source[15] (where the primary source refers to the applied electric field).

This mechanism of virtual electrode generation during field stimulation is illustrated in Fig. 5b, which shows the different activation patterns associated with two inexcitable circular obstacles in idealized simulated atrial tissue as the electrical field strength is increased. The activating shock was delivered by injecting current from the positive electrode (left), which passed through the tissue and exited at the negative electrode (right). At the lowest field strength, only the tissue edge (which constitutes a large conductivity discontinuity) became an activation site. As the electric field strength was increased, tissue near the boundary of the larger obstacle was activated. With a further increase in the field strength, tissue near the boundary of the smaller obstacle was activated as well. Although the entire right edge of the tissue was depolarized, it was the tissue abutting not the right, but the left edges of the obstacles that was depolarized, in accordance with Fig. 5a.

A similar pattern was observed in the more anatomically realistic setting of Fig. 5c and d. In this case, two regions of an arterially perfused canine ventricular preparation were subjected to cryoablation to create marked conductivity discontinuities. In Fig. 5c, a computer simulation of the effects of field stimulation in this setting was conducted using a two-dimensional ventricular slice digitized from this experimental preparation. As in Fig. 5b, at the lowest electric field strength, only the tissue edge closest to the negative electrode was activated. As the field strength was increased, additional activations originated from the edges of the conductivity discontinuities closer to the positive electrode. The same effects were seen in the actual experimental setting in Fig. 5d and the related movies. As in Fig. 5b and c, the lowest field strength (0.18 V/cm) activated only the tissue edge closest to the negative electrode. At a field strength of 0.56 V/cm, not only was a larger area of activation produced at the lower edge of the preparation, but activations also were initiated near the edges of the cryoablated regions closer to the positive electrode, as in the simulations. However, unlike the two-dimensional simulations, in three-dimensional tissue activations eventually were seen within the cryoablated regions as well, most likely because the cryoablated areas were not completely transmural. Consequently, tissue below the surface, which was still viable, produced an optical signal.[33] At a field strength of 0.93 V/cm, more tissue around the conductivity discontinuities and at the tissue edges was activated and optical signals from the cryoablated areas were even more pronounced. Figure 6 shows simulated atrial tissue simulations where collagenous septa and gap junction conductivity discontinuities were incorporated to represent the insulating plaques that typically form between fibers in older hearts.[31] Figure 6b demonstrates how in this setting the number of activation sites produced by the conductivity discontinuities increased as the field strength was increased from 0.8 to 1.14 V/cm. In addition, the time required to depolarize the entire tissue decreased with increasing field strength, as shown in Fig. 6c for simulated tissue and in Fig. 7 for actual atrial tissue.

Unlike in the experimental preparations, where it was not technically feasible to detect virtual electrode formation during FF-AFP, in the computer simulations it was clear, as shown in Fig. 6d and the related movie, that FF-AFP generated multiple activation sites at conductivity discontinuities, thereby progressively entraining the entire tissue and terminating the arrhythmia with repeated pulse application. In this case, three reentrant waves were terminated after eight successive monophasic shocks of 5 ms duration at a cycle length matching the spiral wave period.

Discussion

We have demonstrated a new method to terminate fast atrial tachycardias and AF. In this method, electrodes located at a small distance from the heart deliver a train of low-voltage shocks at a rapid rate. Our data are consistent with the idea that during the low-energy shocks, small intrinsic conductivity discontinuities behave as internal “virtual” electrodes.[16-23] The virtual electrodes serve as activation sites (or secondary sources) if the field strength depolarizes the tissue beyond the excitation threshold.[15,16] At very low field strengths, only a single virtual pacing site may be created, whereas at slightly higher field strengths, many more activation sites arise and the time required to excite a given myocardial preparation decreases[16] (see Fig. 7f). The more virtual electrodes recruited during FF-AFP, the easier it is to entrain the entire tissue and to terminate an arrhythmia.

In a previous study Ripplinger et al.[25] demonstrated that a precisely timed low-voltage electric field could detach a pinned reentrant wave and move it to a boundary for extinction. Although this method is likely to be effective for terminating an arrhythmia arising from a single reentrant source, multiple stimuli applied at numerous sites are required to terminate fibrillation using this phase-coupled approach.[14] As in the Ripplinger et al.[25] study, FF-AFP uses an electric field to create activation at a conductivity discontinuity, but the timing of the introduction of

the field is not critical, in that the objective is not to unpin waves and move them to a boundary, but rather to entrain progressively larger regions of tissue. Consequently, FF-AFP is capable of terminating multiple anatomical and functional reentries simultaneously, without moving them to boundaries (see Fig. S3 and the related movie), and may, therefore, be a useful approach for terminating polymorphic tachycardias and fibrillation.

The FF-AFP technique represents an innovative approach to the treatment of AF. Pharmacological therapy is not always successful in terminating atrial arrhythmias or in preventing them from recurring with increasing frequency.[3] Other forms of electrical intervention also have a number of limitations. Catheter ablation approaches, for example, while successful in some patient populations,[34] have not been shown to be effective for a broad range of patients.[3] Because of its restriction to a single site, ATP requires a frequency fast enough to extinguish, rather than simply entrain, reentrant waves,[10] as the electrode may lie outside the core of the reentrant wave(s). These rapid rates can increase the likelihood of inducing AF.[35] Cardioversion using implantable cardioverter defibrillators successfully terminates 90% of paroxysmal AF and 75% of persistent AF with biphasic shocks (~3ms/3ms) with mean threshold energies of 7 J.[7,36,37] However, such high-energy shocks produce considerable discomfort in patients[38,39] and damage the myocardium.[40]

Our findings show that FF-AFP has many of the advantages of ATP and cardioversion and fewer of the drawbacks. Specifically, it duplicates the significant success rate of cardioversion (93% in our *in vitro* experiments), while avoiding damaging high-energy shocks. Moreover, FF-AFP is unique in that it is not simply a modification of either ATP or cardioversion. It relies on low-strength electric fields to induce activations at conductivity discontinuities throughout the tissue. These activation sites have an increased likelihood of generating an excitation that will affect reentrant waves, or more specifically, the excitable gaps between waves, with more nearly synchronous timing. As a result, the excitable gaps are filled almost simultaneously and completely and because the tissue is fully captured at the FF-AFP pacing cycle length, rotating waves are terminated. With the extinction of reentry, normal sinus rhythm can resume.

In addition to discontinuities in conductivity, dynamical heterogeneities arising from dispersion of repolarization during fibrillation potentially could act as virtual electrodes, especially along activation wavefronts, where the voltage gradients are steepest. However, our computer modeling studies indicate that the effects of electric fields on these dynamical discontinuities, during fibrillation, are much smaller than those on static conductivity discontinuities (as shown in Fig. S4).

The energy needed for successful defibrillation using FF-AFP ranged between 0.074 and 0.81 J, with an average of 0.24 J, which is below the energy where sedation is necessary (0.5 to 1 J).[38,39] Although the average energy for termination by FF-AFP in our *in vitro* model is below the pain threshold (0.4 J),[41] the number of FF-AFP shocks could affect pain perception, in that a series of shocks seems more painful than one shock and subsequent shocks subjectively feel stronger, even when they are less strong than previous shocks.[7] Nevertheless, it is expected that the use of biphasic, truncated, and other waveforms, instead of the monophasic waveforms used in this study, together with optimized geometry and placement of electrodes,[37] will further decrease the required FF-AFP energies, possibly to levels below the threshold for pain perception. For instance, biphasic cardioversion shocks with an 80 percent success rate require less than one-third the energy needed to achieve a similar success rate using monophasic shocks.[6] Additionally, AFP may be more effective in older patients and patients with fibrosis or scarring because of the higher incidence of conductivity discontinuities these patients are likely to possess,[31] therefore potentially increasing the number of virtual electrodes recruited and further reducing the energy required for successful cardioversion. Addressing these issues and future clinical relevance will require further studies of the efficacy of FF-AFP *in vivo.*

Clinical Summary

This study tested whether low-amplitude shocks delivered via two field electrodes were capable of terminating atrial fibrillation in isolated perfused canine atria. Our expectation was that the fields induced by the two physical electrodes would create many “virtual” electrodes that could then be used to overdrive-pace the fibrillating tissue and thereby terminate fibrillation. The observation that this method, which we call far-field anti-fibrillation pacing (FF-AFP), converted atrial fibrillation reliably (93% success rate) using field strengths that were only 13% of the energy required to cardiovert using a single shock, suggests that this method may have clinical utility. Cardioversion of AF using lower energies could reduce the pain and tissue damage associated with a large single shock and prolong the battery life of implantable devices. Further experimental studies are needed, however, to optimize the shock protocol and to determine whether FF-AFP is effective and safe *in vivo*.

Acknowledgments

We thank M.W. Enyeart and D. Raskolnikov for technical assistance and Giles J. Hooker for statistical consultation.

Funding Sources

This work was supported in part by the National Institutes of Health grants HL075515-S03,-S04 (F.H.F.), HL075515 (R.F.G.), and HL073644 (R.F.G. and E.B.); by IFCPAR Project no. 3404-4 (A.P.) and by National Science Foundation Grants no. 0800793 (F.H.F. and E.M.C.) and no. BES-0503336 (E.B.). S.L. and E.B. acknowledge support from the Max Planck Society. This work also was supported in part by the Kavli Institute for Theoretical Physics under National Science Foundation grant PHY05-51164 and by the National Science Foundation through TeraGrid resources provided by the Pittsburgh Supercomputing Center.

References

1. Waktare JE. Cardiology patient page. Atrial fibrillation. Circulation 2002;106:14–16. [PubMed: 12093762]
2. Heart Disease and Stroke Statistics—2007 Update. Circulation 2007;115:e69–e171. [PubMed: 17194875]
3. Nattel S, Opie LH. Controversies in atrial fibrillation. Lancet 2006;367:262–272. [PubMed: 16427496]
4. Wijffels M, Kirchhof C, Dorland R, Allessie MA. Atrial fibrillation begets atrial fibrillation: a study in awake chronically instrumented goats. Circulation 1995;92:1954–1968. [PubMed: 7671380]
5. Ideker RE, Zhou X, Knisley SB. Correlation among fibrillation, defibrillation, and cardiac pacing. Pacing Clin Electrophysiol 1995;18:512–525. [PubMed: 7777416]
6. Koster RW, Dorian P, Chapman FW, Schmitt PW, O'Grady SG, Walker RG. A randomized trial comparing monophasic and biphasic waveform shocks for external cardioversion of atrial fibrillation. Am Heart J 2004;147:e20–e26. [PubMed: 15131555]
7. Santini M, Pandozi C, Altamura G, Gentilucci G, Villani M, Scianaro MC, Castro A, Ammirati F, Magris B. Single shock endocavitary low energy intracardiac cardioversion of chronic atrial fibrillation. J Interv Card Electrophysiol 1999;3:45–51. [PubMed: 10354975]
8. Walcott GP, Killingsworth CR, Ideker RE. Do clinically relevant transthoracic defibrillation energies cause myocardial damage and dysfunction? Resuscitation 2003;59:59–70. [PubMed: 14580735]
9. Gillis AM, Unterberg-Buchwald C, Schmidinger H, Massimo S, Wolfe K, Kavaney DJ, Otterness MF, Hohnloser SH, GEM III AT Worldwide Investigators. Safety and efficacy of advanced atrial pacing therapies for atrial tachyarrhythmias in patients with a new implantable dual chamber cardioverter-defibrillator. J Am Coll Cardiol 2002;40:1653–1659. [PubMed: 12427419]
10. Ricci RP. Atrial tachyarrhythmia prevention and treatment by means of special pacing algorithms. Ital Heart J 2005;6:200–205. [PubMed: 15875509]

11. Israel CW, Hügl B, Unterberg C, Lawo T, Kennis I, Hettrick D, Hohnloser SH, AT500 Verification Study Investigators. Pace-termination and pacing for prevention of atrial tachyarrhythmias: results from a multicenter study with an implantable device for atrial therapy. J Cardiovasc Electrophysiol 2001;12:1121–1128. [PubMed: 11699520]
12. Ricci R, Pignalberi C, Disertori M, Capucci A, Padeletti L, Botto G, Toscano S, Miraglia F, Grammatico A, Santini M. Efficacy of a dual chamber defibrillator with atrial antitachycardia functions in treating spontaneous atrial tachyarrhythmias in patients with life-threatening ventricular tachyarrhythmias. Eur Heart J 2001;3:25–32.
13. Allessie M, Kirchhof C, Scheffer GJ, Chorro F, Brugada J. Regional control of atrial fibrillation by rapid pacing in conscious dogs. Circulation 1991;84:1689–1697. [PubMed: 1914108]
14. Pak HN, Liu YB, Hayashi H, Okuyama Y, Chen PS, Lin SF. Synchronization of ventricular fibrillation with real-time feedback pacing: implication to low-energy defibrillation. Am J Physiol Heart Circ Physiol 2003;285:H2704–2711. [PubMed: 12893637]
15. Plonsey R. The nature of sources of bioelectric and biomagnetic fields. Biophys J 1982;39:309–312. [PubMed: 7139030]
16. Fast VG, Rohr S, Gillis AM, Kléber AG. Activation of cardiac tissue by extracellular electrical shocks. Formation of 'secondary sources' at intercellular clefts in monolayers of cultured myocytes. Circ Res 1998;82:375–385. [PubMed: 9486666]
17. Sharifov OF, Fast VG. Optical mapping of transmural activation induced by electrical shocks in isolated left ventricular wall wedge preparations. J Cardiovasc Electrophysiol 2003;14:1215–1222. [PubMed: 14678138]
18. Sambelashvili AT, Nikolski VP, Efimov IR. Virtual electrode theory explains pacing threshold increase caused by cardiac tissue damage. Am J Physiol Heart Circ Physiol 2004;286:H2183–H2194. [PubMed: 14726298]
19. Windisch H, Platzer D, Bilgici E. Quantification of shock-induced microscopic virtual electrodes assessed by subcellular resolution optical potential mapping in guinea pig papillary muscle. J Cardiovasc Electrohysiol 2007;18:1086–1094.
20. Hooks DA, Tomlinson KA, Marsden SG, LeGrice IJ, Smaill BH, Pullan AJ, Hunter PJ. Cardiac microstructure. Implications for electrical propagation and defibrillation in the heart. Circ Res 2002;91:331–338. [PubMed: 12193466]
21. Trayanova N, Skouibine K. Modeling defibrillation: effects of fiber curvature. J Electrocardiol 1998;31(Suppl):23–29. [PubMed: 9988001]
22. Roth BJ, Wikswo JP Jr. A bidomain model for the extracellular potential and magnetic field of cardiac tissue. IEEE Trans Biomed Eng 1986;33:467–469. [PubMed: 3957401]
23. Plank G, Prassl A, Hofer E, Trayanova NA. Evaluating intramural virtual electrodes in the myocardial wedge preparation: simulations of experimental conditions. Biophys J 2008;94:1904–1915. [PubMed: 17993491]
24. Pumir A, Nikolski V, Hörning M, Isomura A, Agladze K, Yoshikawa K, Gilmour R, Bodenschatz E, Krinsky V. Wave emission from heterogeneities opens a way to controlling chaos in the heart. Phys Rev Lett 2007;99:208101. [PubMed: 18233188]
25. Ripplinger CM, Krinsky VI, Nikolski VP, Efimov IR. Mechanisms of unpinning and termination of ventricular tachycardia. Am J Physiol Heart Circ Physiol 2006;291:H184–192. [PubMed: 16501014]
26. Fedorov VV, Lozinsky IT, Sosunov EA, Anyukhovsky EP, Rosen MR, Balke W, Efimov IR. Application of blebbistatin as an excitation-contraction uncoupler for electrophysiogic study of rat and rabbit hearts. Heart Rhythm 2007;4:619–626. [PubMed: 17467631]
27. Allessie MA, Lammers WJ, Bonke IM, Hollen J. Intra-atrial reentry as a mechanism for atrial flutter induced by acetylcholine and rapid pacing in the dog. Circulation 1984;70:123–35. [PubMed: 6723008]
28. Fenton FH, Cherry EM, Karma A, Rappel WJ. Modeling wave propagation in realistic heart geometries using the phase-field method. Chaos 2005;15:013502.
29. Fox JJ, McHarg JL, Gilmour RF Jr. Ionic mechanism of electrical alternans. Am J Physiol Heart Circ Physiol 2002;282:H516–H530. [PubMed: 11788399]

30. Nygren A, Fiset C, Firek L, Clark JW, Lindblad DS, Clark RB, Giles WR. Mathematical model of an adult human atrial cell: the role of K+ currents in repolarization. Circ Res 1998;82:63–81. [PubMed: 9440706]

31. Spach MS, Dolber PC. Relating extracellular potentials and their derivatives to anisotropic propagation at a microscopic level in human cardiac muscle. Circ Res 1986;3:356–371. [PubMed: 3719925]

32. Kneller J, Zou R, Vigmond EJ, Wang Z, Leon LJ, Nattel S. Cholinergic atrial fibrillation in a computer model of a two-dimensional sheet of canine atrial cells with realistic ionic properties. Circ Res 2002;90:e73–e87. [PubMed: 12016272]

33. Bernus O, Wellner M, Mironov SF, Pertsov AM. Simulation of voltage-sensitive optical signals in three-dimensional slabs of cardiac tissue: application to transillumination and coaxial imaging methods. Phys Med Biol 2005;50:215–229. [PubMed: 15742940]

34. Haïssaguerre M, Hocini M, Sanders P, Sacher F, Rotter M, Takahashi Y, Rostock T, Hsu LF, Bordachar P, Reuter S, Roudaut R, Clémenty J, Jaïs P. Catheter ablation of long-lasting persistent atrial fibrillation: clinical outcome and mechanisms of subsequent arrhythmias. J Cardiovasc Electrophysiol 2005;16:1138–1147. [PubMed: 16302893]

35. Waldo A Atrial flutter: entrainment characteristics. J Cardiovasc Electrophysiol 1997;8:337–352. [PubMed: 9083885]

36. Alt E, Schmitt C, Ammer R, Coenen M, Fotuhi P, Karch M, Blasini R. Initial experience with intracardiac atrial defibrillation in patients with chronic atrial fibrillation. Pacing Clin Electrophysiol 1994;17:1067–1078. [PubMed: 7518595]

37. Saksena S, Prakash A, Mangeon L, Varanasi S, Kolettis T, Mathew P, De Groot P, Mehra R, Krol RB. Clinical efficacy and safety of atrial defibrillation using biphasic shocks and current nonthoracotomy endocardial lead configurations. Am J Cardiol 1995;76:913–921. [PubMed: 7484831]

38. Murgatroyd FD, Slade AKB, Sopher M, Rowland E, Ward DE, Camm AJ. Efficacy and tolerability of transvenous low energy cardioversion of paroxysmal atrial fibrillation in humans. J Am Coll Cardiol 1995;25:1347–1353. [PubMed: 7722132]

39. Lévy S. Internal defibrillation: where we have been and where we should be going? J Interv Card Electrophysiol 2005;13(Suppl):61–66. [PubMed: 16133857]

40. Nikolski VP, Sambelashvili AT, Krinsky VI, Efimov IR. Effects of electroporation on optically recorded transmembrane potential responses to high-intensity electrical shocks. Am J Physiol Heart Circ Physiol 2004;286:H412–H418. [PubMed: 14527941]

41. Steinhaus DM, Cardinal DS, Mongeon L, Musley SK, Foley L, Corrigan S. Internal defibrillation pain perception of low energy shocks. Pacing Clin Electrophysiol 2002;25:1090–1093. [PubMed: 12164452]

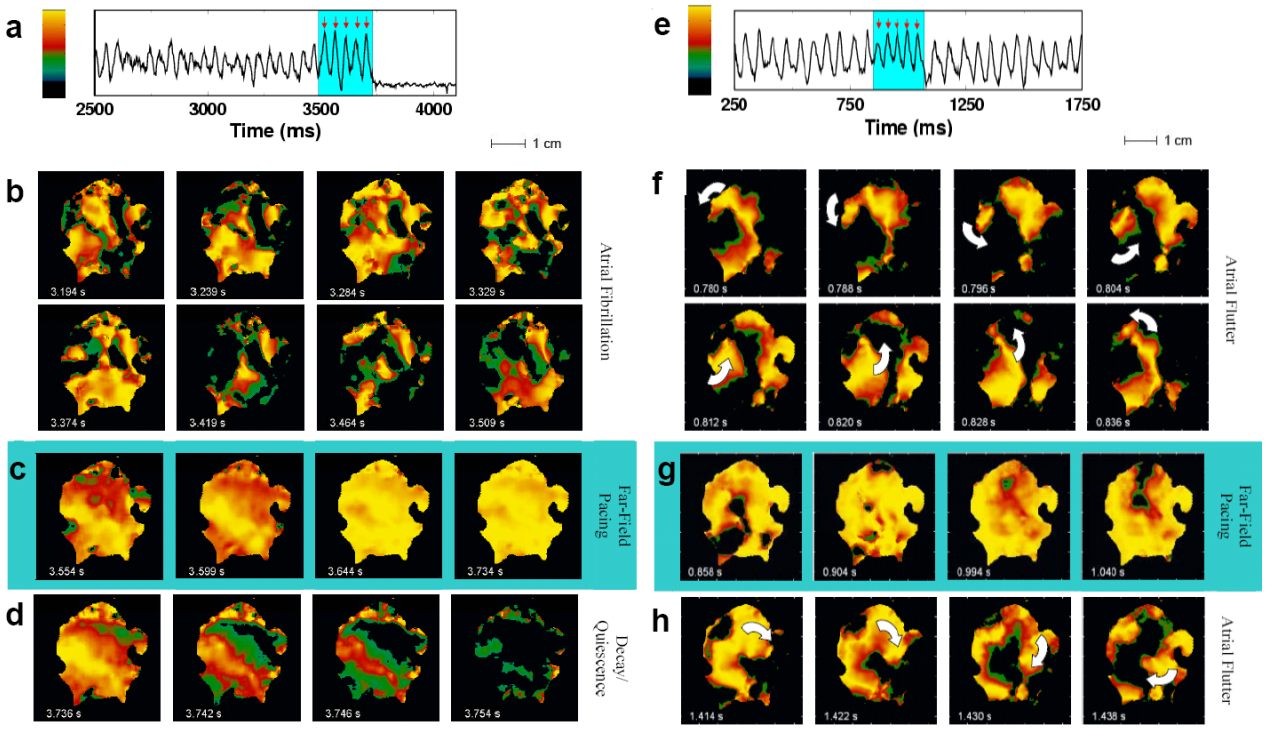

Figure 1.

Successful and unsuccessful termination of AF. **a.** Optical signal from one pixel during AF showing successful defibrillation after delivery of five far-field pulses of 1.4 V/cm at a cycle length of 45 ms (red arrows). **b.** Optical signal during fibrillation; color represents voltage (see color bar in panel a). Frames are 45 ms apart in time and show the complex wave patterns during fibrillation. **c.** Effects of shocks #1, 2, 3 and 5 (left to right), with the first two panels showing partial capture and the last two showing global capture. **d.** Evolution to full repolarization and quiescence following shock #5. **e.** Optical signal from one pixel during atrial flutter showing unsuccessful defibrillation after five field pulses of 0.9V/cm at a cycle length of 45 ms (red arrows). **f.** Optical signal showing a spiral wave rotating counter-clockwise before the shocks. **g.** Partial capture by shocks #1, 2, 4 and 5 (left to right). **h.** Shock-induced conversion of the original spiral wave into a spiral wave rotating clockwise. Throughout, light blue shading indicates time during applied shocks.

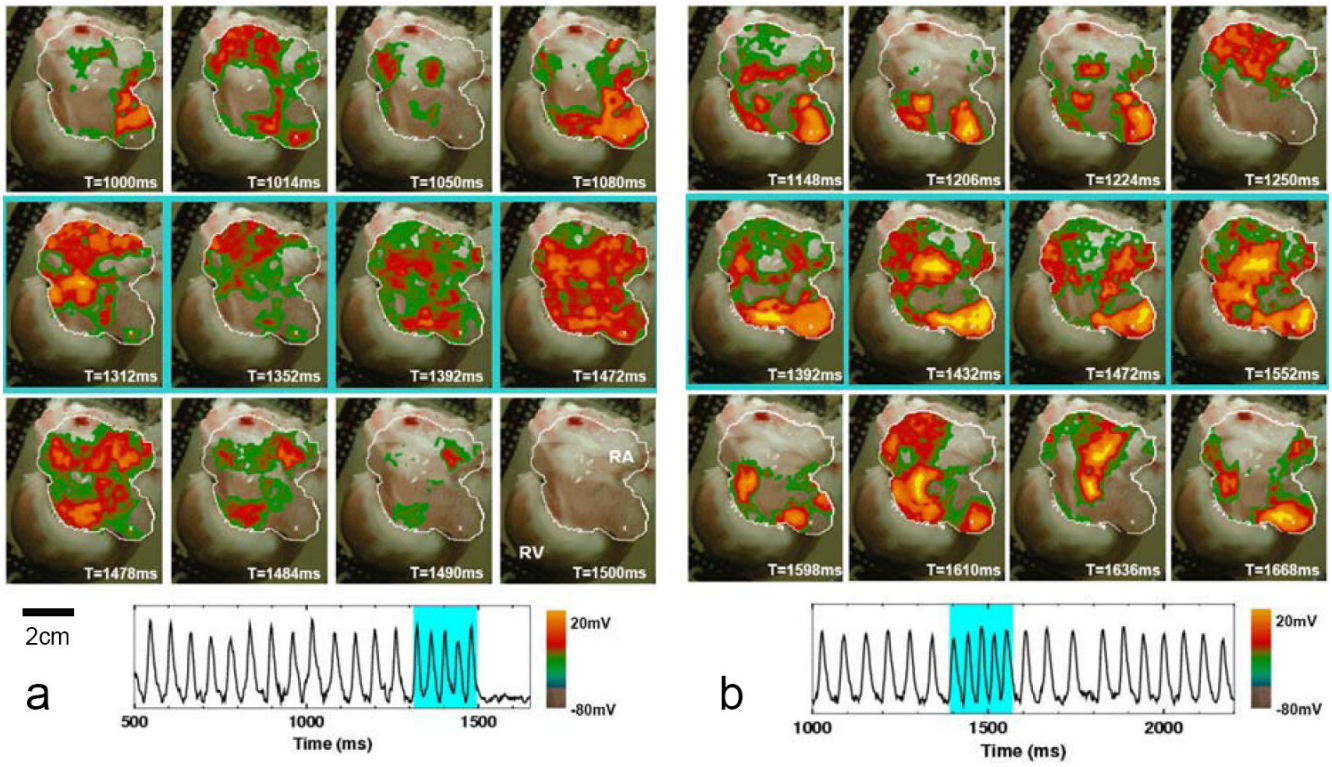

Figure 2.

Successful and unsuccessful termination of atrial fibrillation. **a.** Successful termination. Top row: AF (dominant period = 59 ms) preceding FF-AFP. Middle row: shocks #1, 2, 3, and 5 in a series of 5 electric field pulses 40 ms apart (1.63 V/cm, 5 ms duration). Tissue area captured progressively increases. Bottom row: return to quiescence following the last pulse. Trace shows optical signal from one pixel (white cross in the above panels, lower right) before, during, and after FF-AFP. Light blue shading indicates time during applied shocks. **b.** Unsuccessful termination. Top row: AF (dominant period = 60 ms) preceding FF-AFP. Middle row: shocks #1, 3, 4, and 5 in a series of 5 electric field pulses 40 ms apart (1.40 V/cm, 5 ms duration). Not enough tissue is captured by the last pulse to terminate the arrhythmia. Bottom row: return to AF. Trace shows optical signal from one pixel (white cross in the above panels, lower right) before, during, and after FF-AFP. Light blue shading indicates time during applied shocks.

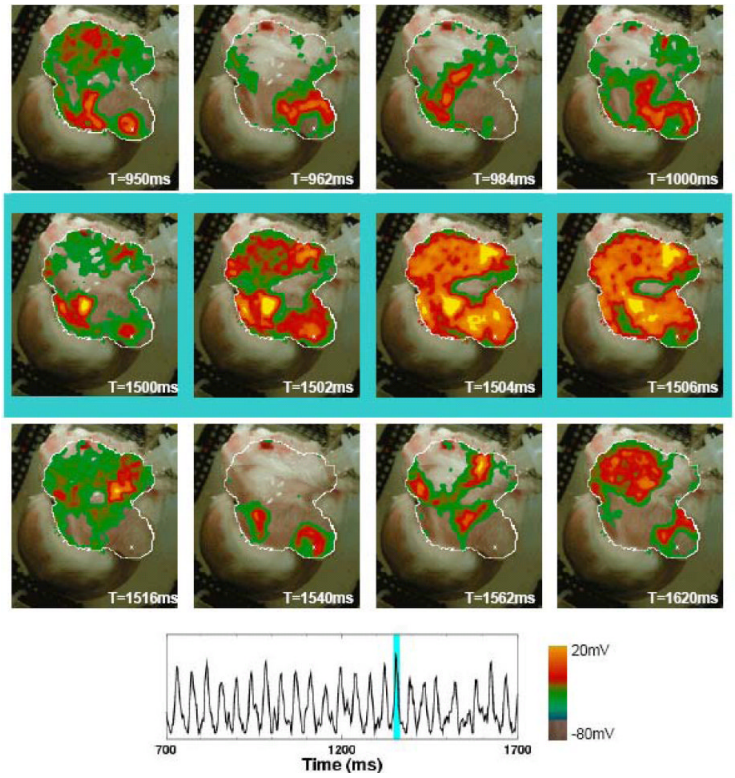

Figure 3.

Unsuccessful termination of AF using a single high-voltage pulse. Top row shows AF preceding application of a single electric field pulse (4.67 V/cm, 5 ms duration), which fails to capture the entire tissue (middle row). Bottom row shows the return to arrhythmia following the pulse. Trace shows optical signal from one pixel (white cross in the above panels, lower right) before, during, and after FF-AFP. Light blue shading indicates time during applied shock. (2 μM ACh).

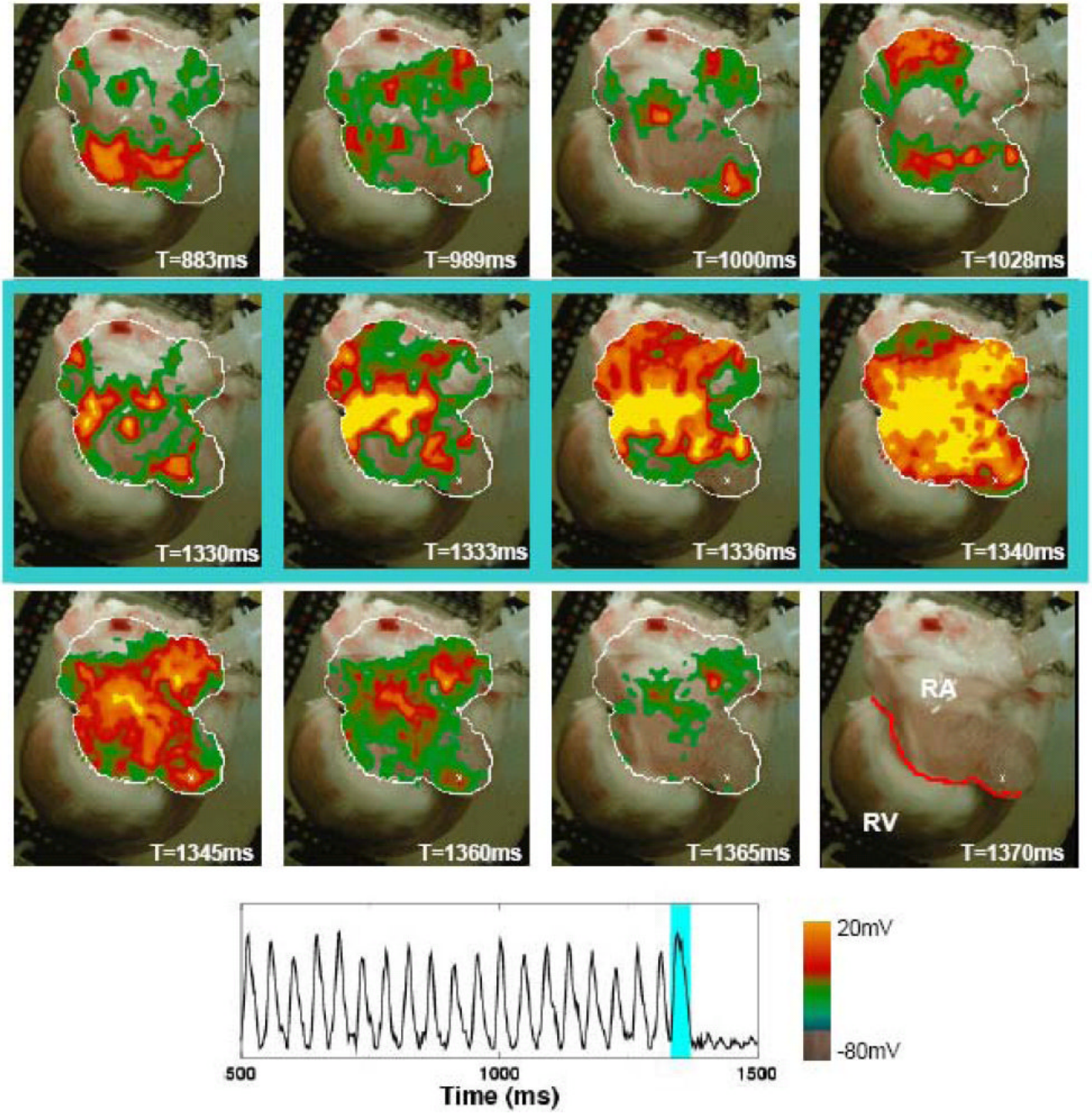

Figure 4.

Successful termination of AF using a single high-voltage pulse. Top row shows AF preceding application of a single electric field pulse (3.73 V/cm, 10 ms duration), which successfully captures the entire tissue (middle row). Bottom row shows quiescence following the pulse. Trace shows optical signal from one pixel (white cross in the above panels, lower right) before, during, and after FF-AFP. The last panel indicates tissue geometry, with the red line separating the right atrium from the right ventricle. Light blue shading indicates time during applied shock. Same preparation as Figure 3 (2 μM ACh).

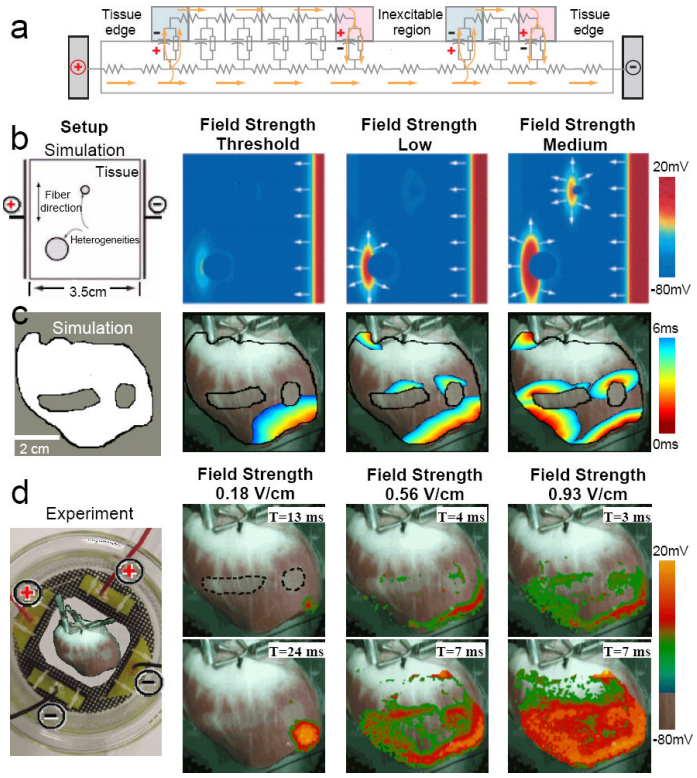

Figure 5.

Mechanism of activation site formation. **a**. Schematic circuit representation of cardiac tissue with an inexcitable obstacle using the bidomain model. Current injected by the positive electrode produces regions of hyperpolarization (blue) and depolarization (red). **b.** Idealized simulated cardiac tissue with conductivity discontinuities created by two inexcitable obstacles. With increasing field strengths, first the tissue edge, then a single conductivity discontinuity, and finally both conductivity discontinuities are excited. Spatial resolution is 250 μm. **c.** Realistic simulated cardiac tissue with two inexcitable obstacles. As in **b**, increasing the field strength recruits more conductivity discontinuities as virtual electrodes. Spatial resolution is 100 μm. **d.** Experimental preparation with two inexcitable obstacles created by cryoablation shown with a dotted line (geometry as in c). Increased field strengths progressively activate more tissue.

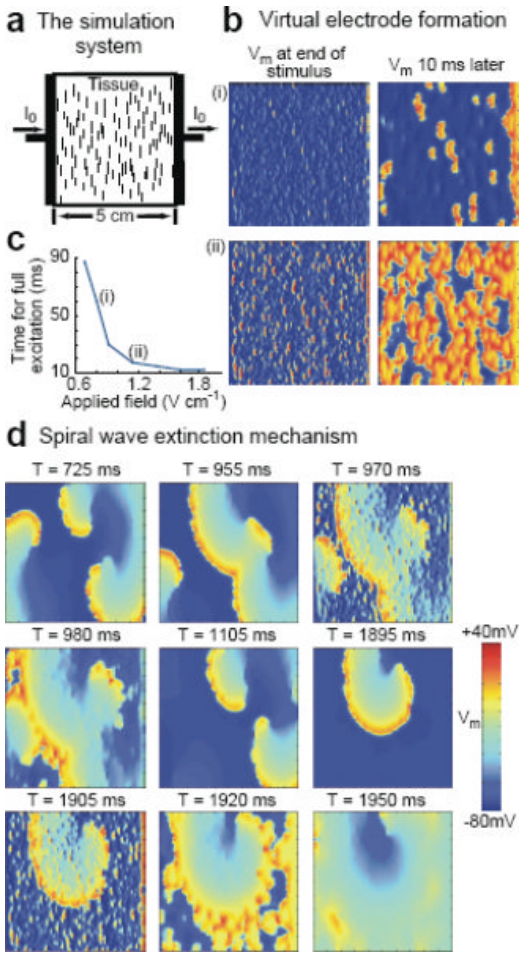

Figure 6.

Simulation of virtual electrode formation and termination of reentry in tissue with multiple small conductivity discontinuities. **a.** Tissue setup schematic. Pacing stimuli are delivered to a square sheet of cardiac tissue by injecting current from the left planar electrode. Collagenous septa (short vertical lines), randomly distributed throughout the tissue, serve as conductivity discontinuities around which induced activations form in response to the applied stimuli. Septa sizes are increased 10 times and only one of every 32 is shown for clarity. Spatial resolution is 250 μm. **b**. Membrane potential V_m induced in the tissue by field strengths of (i) 0.8 V/cm and (ii) 1.14 V/cm (5 ms, square wave pulse). **c**. Time required for a single applied stimulus of various field strengths to depolarize the entire tissue from the resting state. **d**. Termination of reentry by eight low-voltage shocks at a cycle length corresponding to the spiral wave period. Membrane potential is shown before and after shocks #3 and 8 (S3 and S8, delivered at T= 970 ms and T= 1905 ms, respectively).

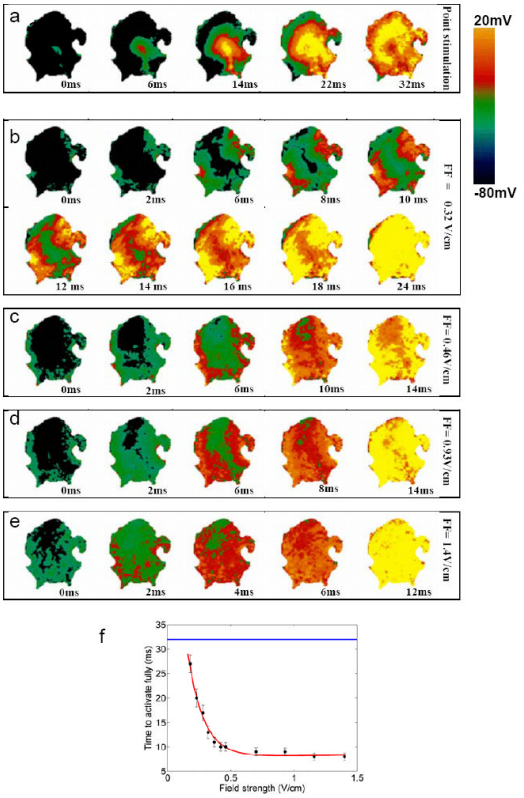

Figure 7.

Recruitment of activation sites as a function of field strength in atrial tissue. **a.** Propagation induced by stimulation using a point electrode. **b-e.** Activation of tissue by field stimulation at field strengths of 0.32, 0.46, 0.93, and 1.4 Vcm. As field strength is increased, more virtual electrodes are recruited, resulting in more rapid depolarization of the entire tissue. **f.** Time to full activation of the tissue as a function of electric field strength. Blue line represents time to full activation from a point stimulus.